

# Study of Materials Deformation in Nanometric Cutting by Large-scale Molecular Dynamics Simulations

Q. X. Pei · C. Lu · H. P. Lee · Y. W. Zhang

Received: 22 December 2008 / Accepted: 27 January 2009 / Published online: 18 February 2009  
© to the authors 2009

**Abstract** Nanometric cutting involves materials removal and deformation evolution in the surface at nanometer scale. At this length scale, atomistic simulation is a very useful tool to study the cutting process. In this study, large-scale molecular dynamics (MD) simulations with the model size up to 10 millions atoms have been performed to study three-dimensional nanometric cutting of copper. The EAM potential and Morse potential are used, respectively, to compute the interaction between workpiece atoms and the interactions between workpiece atoms and tool atoms. The material behavior, surface and subsurface deformation, dislocation movement, and cutting forces during the cutting processes are studied. We show that the MD simulation model of nanometric cutting has to be large enough to eliminate the boundary effect. Moreover, the cutting speed and the cutting depth have to be considered in determining a suitable model size for the MD simulations. We have observed that the nanometric cutting process is accompanied with complex material deformation, dislocation formation, and movement. We find that as the cutting depth decreases, the tangential cutting force decreases faster than the normal cutting force. The simulation results reveal that as the cutting depth decreases, the specific cutting force increases, i.e., “size effect” exists in nanometric cutting.

**Keywords** Molecular dynamics · Nanometric cutting · Materials deformation · Large-scale simulation

## Introduction

Nanometric cutting is a tool-based materials removal technique to remove materials at nanometer scale thickness in the surface. Nanometric cutting can be used to produce micro/nano-components with nanoscale surface finish and sub-micron level form accuracy for many applications such as micro-electro-mechanical systems (MEMS) and nano-electro-mechanical systems (NEMS) [1, 2]. Understanding the material removal mechanism and mechanics at atomistic scale in the surface, such as deformation evolution, chip formation, machined surface, cutting forces, and friction, is a critical issue in producing high precision components. However, as the nanometric cutting process involves only a few atomic layers at the surface, it is extremely difficult to observe the cutting process and to measure the process parameters through experiments. Therefore, theoretical analysis plays a major role in obtaining information on nanometric cutting. The widely used finite element method based on continuum mechanics for the analysis of conventional cutting is not appropriate to analyze the nanometric cutting process because of the discrete nature of materials at such a small length scale; therefore molecular dynamics (MD) simulation has become a very useful tool in the study of nanometric cutting.

A number of studies have used the MD simulations to analyze the nanometric cutting process [3–9]. The typical studies among them include: Maekawa et al. [3] studied the role of friction between a single-crystal copper and a diamond-like tool in nano-scale orthogonal machining. The Morse type potentials were used for the interactions between Cu–Cu, Cu–C, and C–C atoms; Zhang et al. [4] studied the wear and friction on the atomic scale and identified four distinct regimes of deformation consisting

---

Q. X. Pei (✉) · C. Lu · H. P. Lee · Y. W. Zhang  
Institute of High Performance Computing, 1 Fusionopolis Way,  
Singapore 138632, Singapore  
e-mail: peiqx@ihpc.a-star.edu.sg

of no-wear, adherence, plowing, and cutting regimes; Komanduri et al. [5–7] carried out MD simulations of nanometric cutting of single-crystal copper and aluminum. They investigated the effects of crystal orientation, cutting direction and tool geometry on the nature of deformation, and machining anisotropy of the material; more recently, Zhang et al. [9] used MD simulations to study the sub-surface deformed layers in the atomic force microscopy (AFM)-based nanometric cutting process.

All those previous studies have provided much help in understanding nanometric cutting. However, as the MD simulation of nanometric cutting is compute-intensive, small simulation models with a few thousands to tens of thousands of atoms were used in the reported studies to reduce the computing time. Although those small models have provided a lot of information on the nanometric cutting processes, a small model may induce significant boundary effects that make the results unreliable. For example, if the model is not large enough, the widely used fixed-atoms boundary in MD simulations may have strong effect on the dislocation movement and thus will affect the motion of atoms at the cutting surface. Besides, in most of the reported studies, the simulation models are two-dimensional or quasi-three-dimensional (plane strain) due to the limitation on the model size. Therefore, there is a need for large-scale MD simulations of three-dimensional (3D) nanometric cutting processes.

Another limitation of previous studies on MD simulations of nanometric cutting of metals is that the Morse potential has been widely adopted to model the interatomic force between metal atoms. Morse potential is a pair potential which considers only two-body interactions; thus, it provides a rather poor description of the metallic bonding. The strength of the individual bond in metals has a strong dependence on the local environment. It decreases as the local environment becomes too crowded due to the

Pauli's "exclusion principle" and increases near surfaces and in small clusters due to the localization of the electron density. The pair potential does not depend on the environment and, as a result, cannot reproduce some of the characteristic properties of metals, such as the much stronger bonding of atoms near surfaces. The EAM potential, which has been specially developed for metals [10–12], can better describe the metallic bonding. Therefore, the EAM potential gives a more realistic description of the behavior and properties of metals than the Morse potential. Our previous study [13] showed that the two different potentials resulted in quite different simulation results and suggested that the EAM potential should be used in MD simulation of nanometric cutting.

In this article, we present large-scale 3D MD simulations of nanometric cutting of copper. In our simulations, the EAM potential is employed for the interactions between Cu atoms in the workpiece. We first studied the model size effect on the simulation results with three different model sizes of about 2, 4, and 10 million atoms. Then, we used the 4-million-atom model, which is shown to be large enough to eliminate the boundary effect, to study the detailed materials deformation, dislocation movement, and cutting forces during the cutting processes.

### Simulation Models and Conditions

Figure 1a–c show three simulation models for our large-scale MD simulations of nanometric cutting. The workpiece sizes are  $40 \times 20 \times 30$  nm containing 2,053,594 atoms,  $40 \times 40 \times 30$  nm containing 4,098,686 atoms, and  $70 \times 44 \times 40$  nm containing 10,137,600 atoms. The diamond tool contains 8446 carbon atoms. The cutting is along the  $x$  direction, which is taken as the [100] direction of the FCC lattice of copper. The boundary conditions of

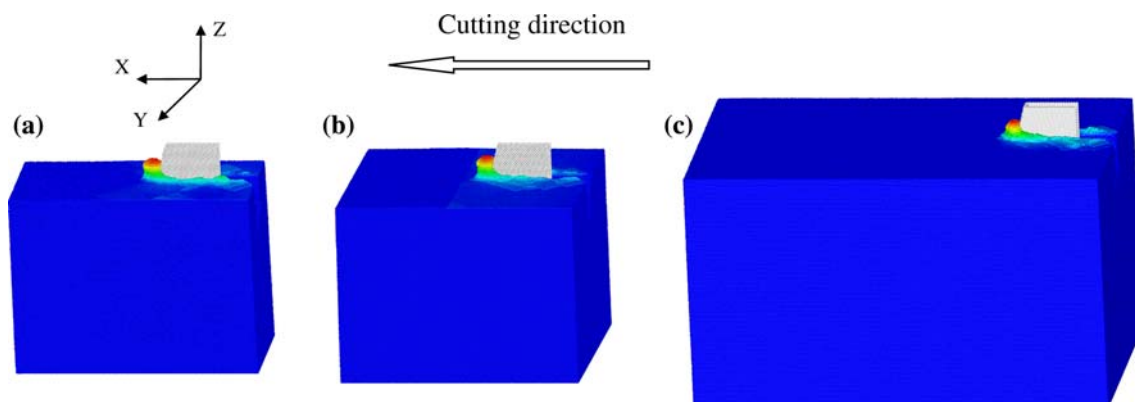


**Fig. 1** The MD simulation models with the number of atoms in the workpiece being around **a** 2 millions, **b** 4 millions and **c** 10 millions. The corresponding workpiece dimensions are  $40 \times 20 \times 30$  nm,

$40 \times 40 \times 30$  nm, and  $70 \times 44 \times 40$  nm, respectively. The cutting tools are in light grey color and the cutting chips ahead the cutting tools are shown in colors ranging from red to light blue

the cutting simulations include: (1) three layers of atoms at the bottom of the workpiece materials (lower  $z$  plane) are kept fixed; (2) periodic boundary conditions are maintained along the  $y$  direction.

In nanometric cutting, as the cutting depth can be as small as a few nanometers, the edge of the cutting tool is not sharp compared with this very small cutting depth. The edge radius of the cutting tool is usually much larger than the cutting depth. Therefore, in our large-scale MD simulations, we use a round edge cutting tool with an edge radius of 6 nm instead of a sharp cutting tool. The geometry of the cutting tool is shown in Fig. 2. The tool thickness is 3.2 nm with the tool rake angle  $\alpha$  and the tool clearance angle  $\beta$  being  $12^\circ$ .

The cutting speed used in the MD simulations ranges from 50 to 500 m/s, while the cutting depth ranges from 0.8 to 4 nm. The cutting is in the (001) plane and along the [100] direction of the workpiece. The initial temperature of the workpiece is 300 K. The three layers of atoms adjacent to the fixed-atom boundary at the workpiece bottom are set as the thermostat atoms, in which the temperatures are maintained at 300 K by rescaling the velocities of the atoms. The velocity Verlet algorithm with a time step of 2 fs is used for the time integration of Newton's equations of motion.

The interatomic forces in MD simulations are calculated from the interatomic potentials. The Morse potential is relatively simple and computationally inexpensive compared to the EAM potential. The Morse potential is as follows:

$$\phi(r_{ij}) = D \{ \exp[-2\alpha(r_{ij} - r_0)] - 2\exp[-\alpha(r_{ij} - r_0)] \} \quad (1)$$

where  $\phi(r_{ij})$  is a pair potential energy function;  $D$  is the cohesion energy;  $\alpha$  is the elastic modulus;  $r_{ij}$  and  $r_0$  are the

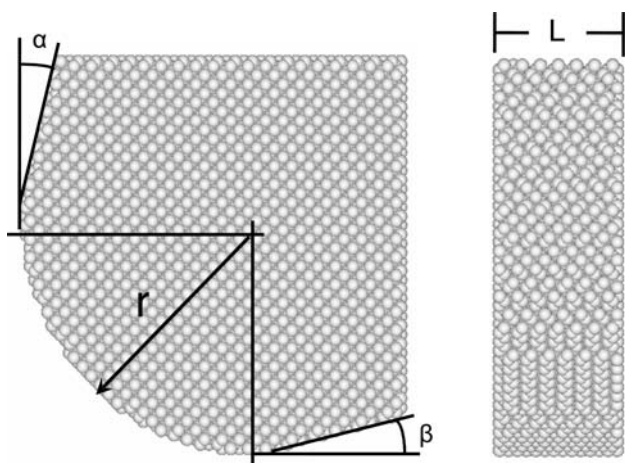


**Fig. 2** The geometry of the cutting tool. The tool edge radius  $r = 6$  nm. The rake angle  $\alpha = 12^\circ$  and clearance angle  $\beta = 12^\circ$ . The tool thickness  $L = 3.2$  nm

instantaneous and equilibrium distance between atoms,  $i$  and  $j$ , respectively.

The EAM method, which has been evolved from the density-function theory, is based upon the recognition that the cohesive energy of a metal is governed not only by the pair-wise potential of the nearest neighbor atoms, but also by embedding energy related to the “electron sea” in which the atoms are embedded. For EAM potential, the total atomic potential energy of a system is expressed by the following equation:

$$E_{tot} = \frac{1}{2} \sum_{ij} \Phi(r_{ij}) + \sum_i F_i(\bar{\rho}_i) \quad (2)$$

where  $\Phi_{ij}(r_{ij})$  is the two-body interaction energy between atoms,  $i$  and  $j$ , with separation distance,  $r_{ij}$ ;  $F_i$  is the embedding energy of atom,  $i$ ;  $\bar{\rho}_i$  is the host electron density at site,  $i$ , induced by all other atoms in the system, which is given by the following equation:

$$\bar{\rho}_i = \sum_{j \neq i} \rho_j(r_{ij}) \quad (3)$$

where  $\rho_j(r_{ij})$  is the contribution to the electronic density at atom,  $i$ , due to atom,  $j$ , at distance,  $r_{ij}$ , from the atom,  $i$ .

There are three different atomic interactions in the MD simulations of nanometric cutting processes: (1) the interaction in the workpiece; (2) the interaction between the workpiece and the tool; and (3) the interaction in the tool. For the interaction between the copper atoms in the workpiece, we used the EAM potential for copper constructed by Johnson [14]. For the interaction between the copper workpiece and the diamond tool, as there is no available EAM potential between Cu and C atoms, we still use the Morse potential for the workpiece–tool interaction with the parameters adopted from reference [4] being  $D = 0.087$  eV,  $\alpha = 5.14$ , and  $r_0 = 2.05$  Å. Since the diamond tool is much harder than the copper workpiece, it is a good approximation to take the tool as a rigid body. Therefore, the atoms in the tools are fixed relative to each other, and no potential is needed for the interaction among the tool atoms.

Dislocations play a crucial role in the plastic deformation of materials. However, accurately identifying dislocations at room temperature in MD simulations is a very difficult task due to thermal vibration of atoms. This might be the reason why almost all the previous MD studies of dislocations were carried out at extremely low temperature of 0 K or 1 K [15–21]. The widely used methods to identify dislocations and other lattice defects in MD simulations are the atomic coordinate number [15], the slip vector [16], and the centro-symmetry parameter [17]. We compared these different methods and found that the methods of atomic coordinate number and the slip vector would become less effective in identifying the lattice

defects at finite temperature due to thermal fluctuations of atoms. Therefore, we have chosen to use the centro-symmetry parameter, which is less sensitive to the temperature increase. In a centro-symmetric material (such as copper and other FCC metals), each atom has pairs of equal and opposite bonds among its nearest neighbors. As the material is distorted, these bonds will change direction and/or length, but they will remain equal and opposite under homogeneous elastic deformation. If there is a defect nearby, however, this equal and opposite relation no longer holds. In a perfect bulk FCC lattice, each atom has 12 nearest-neighbor bonds or vectors. The centro-symmetry parameter for each atom is defined as follows:

$$CSP = \sum_{i=1,6} \left| \vec{R}_i + \vec{R}_{i+6} \right|^2 \quad (4)$$

where  $R_i$  and  $R_{i+6}$  are the vectors corresponding to the six pairs of opposite nearest neighbors in the FCC lattice. By definition, the centro-symmetry parameter is zero for an atom in a perfect FCC material under any homogeneous elastic deformation and non-zero for an atom which is near a defect such as a cavity, a dislocation, or a free surface.

The large-scale MD simulations of nanometric cutting are carried out on the IBM p575 supercomputer at the Institute of High Performance Computing (IHPC). The multi-processor parallel computing is used for the simulations. The parallel computing is realized by using message

passing interface (MPI) library. The calculation time for each simulation case depends on the model size, cutting speed, cutting distance, as well as the number of CPUs used. For example, it took about 3 weeks to finish the simulation run for the 10-million-atom model with the cutting speed of 100 m/s using 32 CPUs.

## Simulation Results

### The Simulation Model Size

For a MD simulation, the larger the model size, the less obvious the boundary effect on the simulation results. However, a very large model will take unnecessarily long computing time. Therefore, it is necessary to study the model size effect, so that we can find a suitable model size for the MD simulations of nanometric cutting. The model size should be moderate with diminished boundary effect on the simulation results.

We first performed MD simulations using the 2-million-atom model in Fig. 1a with a cutting speed of 100 m/s and a cutting depth of 4 nm. The simulation results of the 2-million-atom model are shown in Fig. 3a, from which one can see that the lattice defects generated from the cutting exist in the whole subsurface region between the periodic boundaries (see the front view). The centro-symmetry

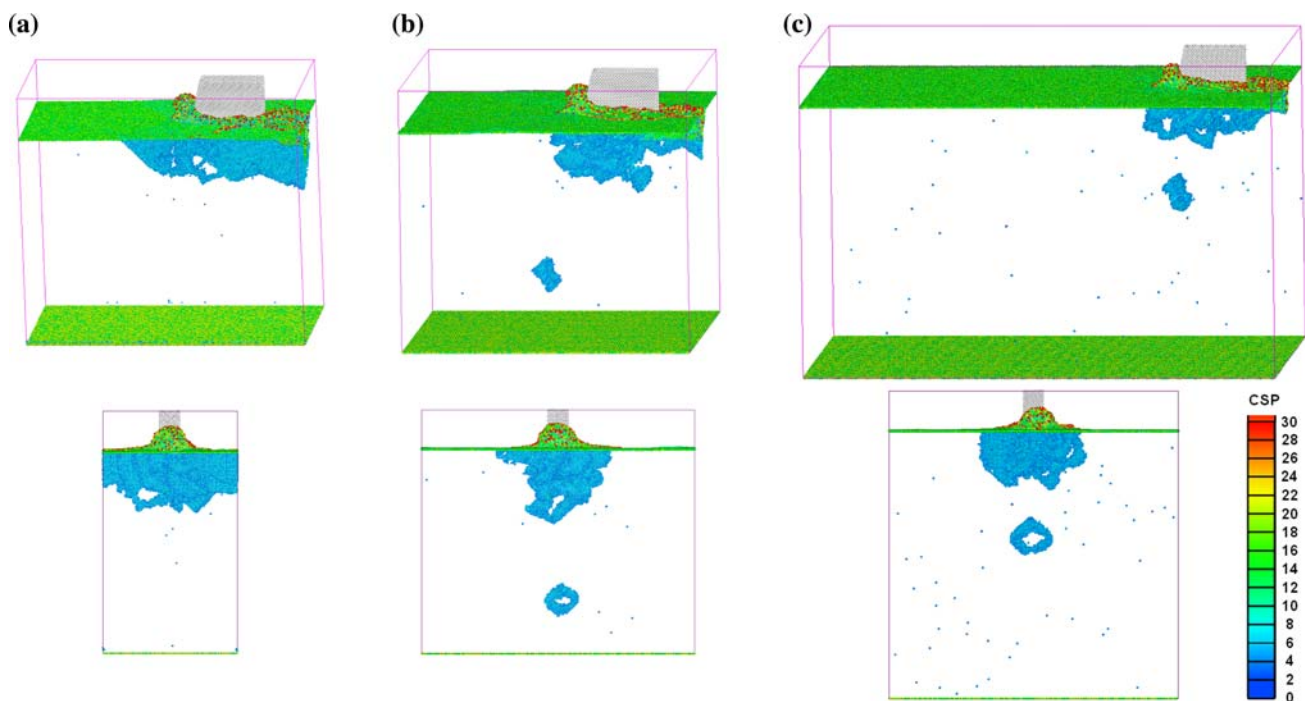


**Fig. 3** The simulation results of the different model sizes: **a** 2-million-atom model, **b** 4-million-atom model and **c** 10-million-atom model. The lower figures are front views of the models. The cutting depth is 4 nm

and the cutting speed is 100 m/s. The blue color shows the dislocations formed inside the workpieces during cutting

parameter (CSP) is used to identify the lattice defects. In Fig. 3a–c, the atoms inside the model with CSP smaller than three are all eliminated in the visualizations, as these atoms are assumed to be in perfect FCC configuration. Note that the isolated atoms distributed inside the model are not lattice defects. Those atoms having CSP above three are due to the thermal vibration of atoms at finite temperature. The periodic boundary condition in  $y$  direction implies that both the workpiece and the cutting tool repeat in this direction. The repeated cutting tools may make the stresses at the periodic boundary regions higher due to stress superposition arising from the interaction of stress fields. The stress interaction is helpful for the dislocations in the cutting regions to slide to the periodic boundaries and also helpful for new dislocations to be generated at the periodic boundaries. This phenomenon was also reported by Saraev et al. [21] in their study of the nanoindentation of copper. As lattice defects exist in the periodic boundaries in the simulation results, the 2-million-atom model is not large enough to eliminate the boundary effect at the periodic boundaries, though it is quite large compared with the models used in the reported works on MD simulation of nanometric cutting.

Thereafter, we performed simulations using the 4-million-atom model in Fig. 1b with the workpiece thickness ( $y$  direction) two times that of the 2-million-atom model. The simulation results in Fig. 3b show that the 4-million-atom model could eliminate the boundary effect of the periodic boundaries. We also carried out simulations with the 10-million-atom model in Fig. 1c. In the 10-million-atom model, the workpiece is larger than that of the 4-million-atom model in all the three dimensions with very obvious increase in both the  $x$  and  $z$  directions to test the boundary effects in these two directions. We found that the simulation results with the 10-million-atom model, shown in Fig. 3c, did not show obvious difference from those of the 4-million-atom model. Therefore, for the cutting speed of 100 m/s and cutting depth of 4 nm, the 4-million-atom-model is shown to

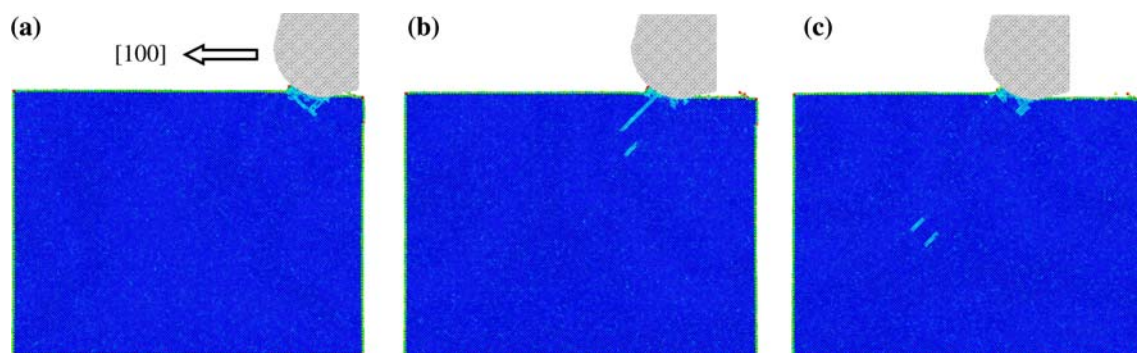
be large enough to ignore the boundary effect in the simulations.

MD simulations were also carried out to study the effect of cutting speed and cutting depth on the boundary effect. The simulation results show that reducing cutting speed results in more obvious boundary effect, while reducing cutting depth results in less obvious boundary effect. This is because a slower cutting speed means longer cutting time, and therefore the dislocations have more time to move and are more possible to reach the boundaries, which makes the boundary effect stronger. A smaller cutting depth means less material deformation, and therefore results in a weaker boundary effect. As the cutting speed and cutting depth may make the boundary effect stronger, it is important to consider those process parameters in choosing the model size for MD simulations of nanometric cutting.

#### Material Deformation, Dislocations, and Cutting Forces

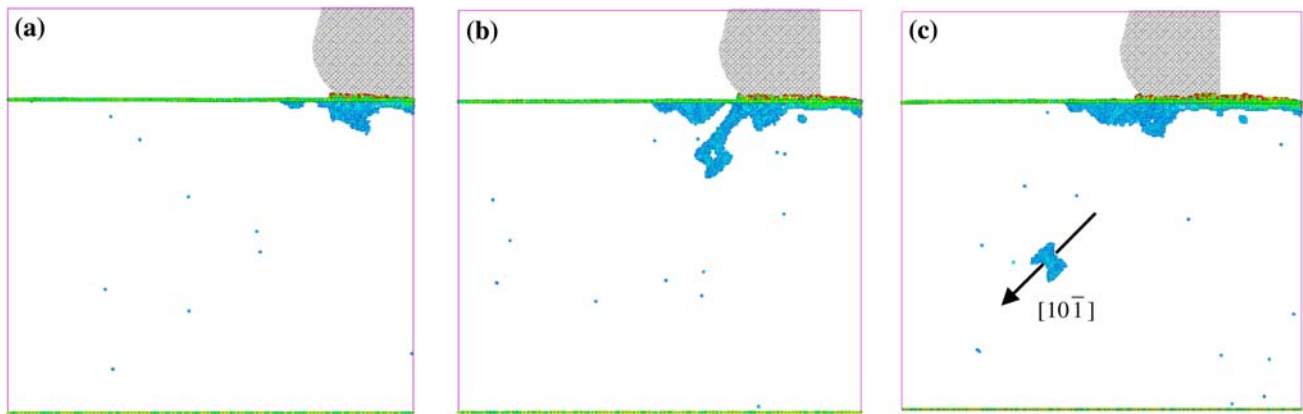
We now analyze the nanometric cutting process of the 4-million-atom model. Figure 4a–c show the cross-sectional views of the  $x$ – $z$  plane at three different cutting distances of 8, 12, and 16 nm, respectively. In this simulation case, the cutting speed is 100 m/s and the cutting depth is 0.8 nm. It can be seen from the figures colored by CSP that the workpiece materials deform during cutting and the material removal takes place via the chip formation as in conventional cutting. The materials in front of and beneath the tool are away from the perfect FCC lattice. Dislocations and other lattice defects are generated in these regions. It can be clearly observed that the dislocations emit from the cutting region and some of them glide deep into the workpiece.

Figure 5a–c present the side views of the 3D lattice defects at the cutting distances of 8, 12, and 16 nm, respectively. In the figures, the defect-free atoms in the workpiece are removed from the visualization. Note that the isolated atoms distributed inside the model are not



**Fig. 4** The simulated nanometric cutting process at the cutting distances of (a) 8 nm, (b) 12 nm and (c) 16 nm. The cutting depth is 0.8 nm and cutting speed is 100 m/s. The figures are shown in the

cross-sectional views. The light blue color shows the cutting chips and dislocations inside the workpiece



**Fig. 5** Side views of the lattice defects during the nanometric cutting process at the cutting distances of (a) 8 nm, (b) 12 nm and (c) 16 nm. The formation and movement of a dislocation loop inside the workpiece can be clearly seen

lattice defects. They are left in the figures due to the thermal vibration of atoms. Although the CSP method is not perfect in identifying the lattice defects at finite temperature, it is more accurate than other methods such as the atomic coordinate number and the slip vector. It can be seen from Fig. 5a–c that lattice defects are formed in the workpiece during the cutting process. Moreover, a dislocation loop is generated and moves in the  $[10\bar{1}]$  direction.

The cutting forces in the MD simulations are obtained by summing the atomic forces of all the workpiece atoms on the tool atoms. The variations of the cutting forces with the cutting distance during the cutting process for this simulation case are shown in Fig. 6. It can be seen that both the tangential cutting force,  $F_x$ , and the normal cutting force,  $F_z$ , increase at the start of the cutting. Then the cutting forces tend to remain steady during the rest of the cutting process. The formation of dislocations results in the release of the accumulated cutting energy, which corresponds to the temporary drop of the cutting force. The fluctuation of the cutting forces in Fig. 6 is due to the formation of dislocations and their complex local

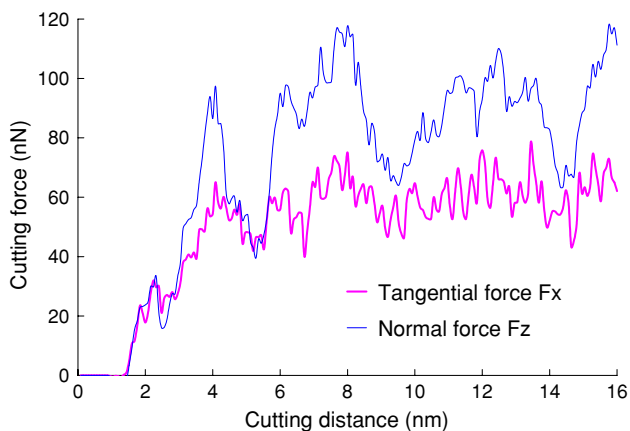


**Fig. 6** Variations of the cutting forces with the cutting distance

movement in the cutting region. It is also observed from Fig. 6 that the normal cutting force,  $F_z$ , shows stronger fluctuation than the tangential cutting force,  $F_x$ . This is because at this very small cutting depth, the normal cutting force is higher than the tangential cutting force, and therefore the normal cutting force undergoes stronger fluctuation. With a larger cutting depth as discussed in next section, the magnitude of normal cutting force is close to that of the tangential cutting force, and so magnitude of the force fluctuations is also close. The simulated cutting force in the thickness direction of the workpiece ( $y$  direction) is not shown here as it is very small with its time-averaged value over the whole cutting process being zero.

#### Effect of Cutting Depth on the Cutting Process

For nanometric cutting, it is interesting to understand how the cutting depth influences the cutting process. Figure 7a–c show material deformation, chip formation, and dislocations during the cutting process for the cutting depths of 0.8, 2.0, and 4.0 nm, respectively. It can be seen that a larger cutting depth results in more workpiece material deformation around the tool and bigger cutting chip. Moreover, a larger cutting depth results in more lattice defects and dislocations in the cutting regions. However, the isolated dislocation loops is not observed in the cutting process for the cutting depth of 2.0 nm, though they are observed for the cutting depths of 0.8 and 4.0 nm. This shows that the dislocation activity is very complex in the nanoscale cutting process.

Figure 8 shows the time-averaged tangential and normal cutting forces during the cutting process for the different cutting depths. It can be seen that both tangential and normal cutting forces decrease as the cutting depth decreases. However, the tangential cutting force decreases faster than the normal cutting force. Consequently, the ratio of normal force to tangential force changes from smaller

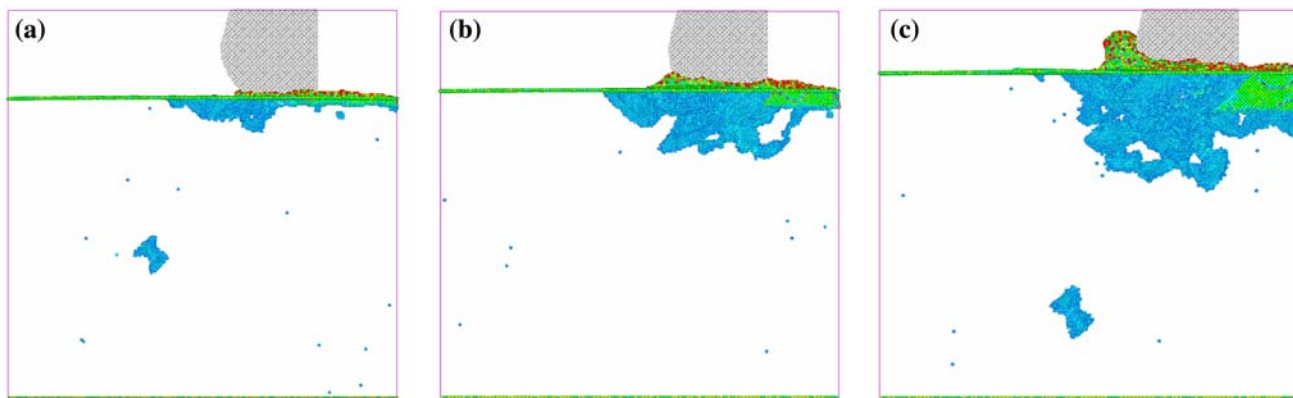


**Fig. 7** Material deformation and dislocations for the cutting depths of (a) 0.8 nm, (b) 2.0 nm and (c) 4.0 nm. The blue color shows the dislocations inside the workpieces

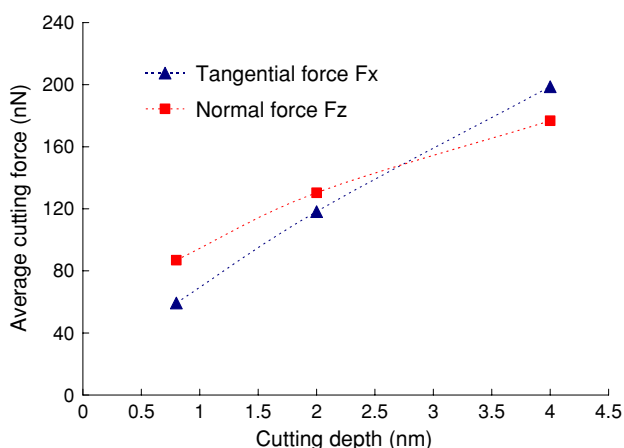


**Fig. 8** Variations of the time-average cutting forces with the cutting depth

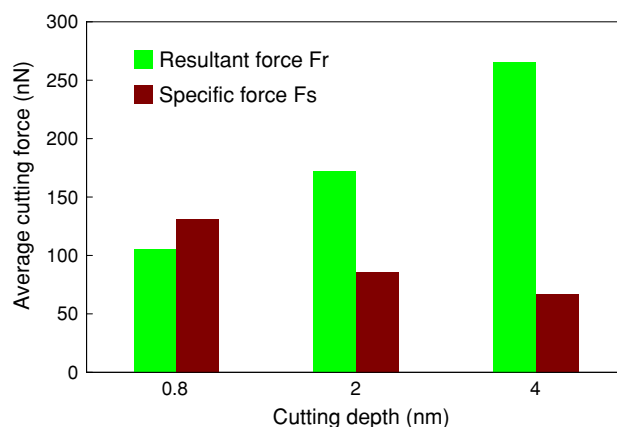


**Fig. 9** The resultant cutting force and the specific cutting force for the different cutting depths of 0.8, 2.0 and 4.0 nm

than 1.0 for the cutting depth of 4.0 nm to greater than 1.0 for the cutting depths of 2.0 and 0.8 nm. This shows that for nanoscale cutting with small cutting depth, as the tool edge radius is quite large compared to the cutting depth, the nanoscale cutting is more similar to the conventional grinding with a large negative tool rake angle.

Figure 9 shows the variations of the resultant cutting force and the specific cutting force with cutting depth. Here the resultant cutting force,  $F_r$ , is the vector sum of the tangential force,  $F_x$ , and normal force,  $F_z$ . Note that the average cutting force along the thickness direction  $F_y$  is zero. The specific cutting force,  $F_s$ , is the resultant cutting force divided by the cutting depth. It can be seen that with the decrease of cutting depth the resultant cutting force decreases. However, the specific cutting force increases rapidly with the decrease of cutting depth, which shows a very obvious “size effect”. The “size effect” on the specific cutting force in nanometric cutting can be explained by the metallic bonding. The special feature of metallic bonding is that the strength of the individual bond has a

strong dependence on the local environment. The bonding becomes stronger at the surface due to the localization of the electron density. The smaller the cutting depth, the larger the ratio of cutting surface to cutting volume, and thus the bigger the specific cutting force.

## Conclusions

We have performed a series of large-scale 3D MD simulations using the EAM potential to study the nanometric cutting process. Three different model sizes of 2-million-atom, 4-million-atom, and 10-million-atom are used with different cutting speeds and cutting depths. It is shown that the 2-million-atom model, though quite large compared with the models used in the previously reported studies, is not large enough to eliminate the boundary effect for the simulation conditions used. It is also shown that the 4-million-atom model is large enough to eliminate the boundary effect at the cutting speed of 100 m/s and cutting

depth of up to 4 nm. A detailed study on the material deformation, lattice defects, dislocation movement, and cutting forces during the cutting process is made with the 4-million-atom model. It is observed that the nanometric cutting process is accompanied by complex material deformation, chip formation, lattice defect generation, and dislocation movement. It is found that as the cutting depth decreases, both the tangential and normal cutting forces decrease; however, the tangential cutting force decreases faster than the normal cutting force. It is also found that as the cutting depth decreases, the specific cutting force increases, which reveals that the “size effect” exists in nanometric cutting.

**Acknowledgments** This work has been supported by the Agency for Science, Technology and Research (A\*STAR), Singapore. Thanks also go to the staffs of the Computational Resource Centre at the Institute of High Performance Computing, who have provided the assistance in the large-scale computing and visualization.

## References

1. E. Masayoshi, O. Takahito, MEMS/NEMS by Micro Nanomachining. IEIC Tech. Rep. **103**, 13 (2003)
2. H.W. Schumacher, U.F. Keyser, U. Zeitler, R.J. Haug, K. Ebert, Controlled mechanical AFM machining of two-dimensional electron systems: fabrication of a single-electron transistor. *Physica E* **6**, 860 (2000). doi:10.1016/S1386-9477(99)00230-1
3. K. Maekawa, A. Itoh, Friction and tool wear in nano-scale machining—a molecular dynamics approach. *Wear* **188**, 115–122 (1995). doi:10.1016/0043-1648(95)06633-0
4. L. Zhang, H. Tanaka, Towards a deeper understanding of wear and friction on the atomic scale—a molecular dynamics analysis. *Wear* **211**, 44 (1997). doi:10.1016/S0043-1648(97)00073-2
5. R. Komanduri, N. Chandrasekaran, L.M. Raff, MD simulation of nanoscale cutting of single crystal aluminum—effect of crystal orientation and direction of cutting. *Wear* **242**, 60 (2000). doi:10.1016/S0043-1648(00)00389-6
6. R. Komanduri, N. Chandrasekaran, L.M. Raff, Molecular dynamics simulation of atomic-scale friction. *Phys. Rev. B* **61**, 14007 (2000). doi:10.1103/PhysRevB.61.14007
7. R. Komanduri, N. Chandrasekaran, L.M. Raff, MD simulation of exit failure in nanoscale cutting. *Mater. Sci. Eng. A* **311**, 1 (2001). doi:10.1016/S0921-5093(01)00960-1
8. T.H. Fang, C.I. Weng, Three-dimensional molecular dynamics analysis of processing using a pin tool on the atomic scale. *Nanotechnology* **11**, 148–153 (2000). doi:10.1088/0957-4484/11/3/302
9. J.J. Zhang, T. Sun, Y.D. Yan, Y.C. Liang, S. Dong, Molecular dynamics simulation of subsurface deformed layers in AFM-based nanometric cutting process. *Appl. Surf. Sci.* **254**, 4774 (2008). doi:10.1016/j.apsusc.2008.01.096
10. M.S. Daw, M.I. Baskes, Embedded-atom method: derivation and application to impurities, surfaces, and other defects in metals. *Phys. Rev. B* **29**, 6443 (1984). doi:10.1103/PhysRevB.29.6443
11. M.W. Finnis, J.E. Sinclair, A simple empirical N-body potential for transition metals. *Philos. Mag. A* **50**, 45 (1984). doi:10.1080/01418618408244210
12. M.S. Daw, S.M. Foiles, M.I. Baskes, The embedded-atom method: a review of theory and applications. *Mater. Sci. Rep.* **9**, 251 (1993). doi:10.1016/0920-2307(93)90001-U
13. Q.X. Pei, C. Lu, F.Z. Fang, H. Wu, Nanoscale cutting of copper: a molecular dynamics study. *Comput. Mater. Sci.* **37**, 434 (2006). doi:10.1016/j.commatsci.2005.10.006
14. R.A. Johnson, Analytic nearest-neighbor model for fcc metals. *Phys. Rev. B* **37**, 3924 (1988). doi:10.1103/PhysRevB.37.3924
15. J. Li, K.J. Van Vliet, T. Zhu, S. Yip, S. Suresh, Atomistic mechanisms governing elastic limit and incipient plasticity in crystals. *Nature* **418**, 307 (2002). doi:10.1038/nature00865
16. A. Zimmerman, C.L. Kelchner, J.C. Hamilton, S.M. Foiles, Surface step effects on nanoindentation. *Phys. Rev. Lett.* **87**, 165507 (2001). doi:10.1103/PhysRevLett.87.165507
17. C.L. Kelchner, S.J. Plimpton, J.C. Hamilton, Dislocation nucleation and defect structure during surface indentation. *Phys. Rev. B* **58**, 11085 (1998). doi:10.1103/PhysRevB.58.11085
18. O. Kum, Orientation effects of elastic-plastic deformation at surfaces: nanoindentation of nickel single crystals. *Mol. Simul.* **31**, 115 (2005). doi:10.1080/08927020412331308502
19. Y.H. Lin, S.R. Jian, Y.S. Lai, P.F. Yang, Molecular dynamics simulation of nanoindentation-induced mechanical deformation and phase transformation in monocrystalline silicon. *Nanoscale Res. Lett.* **3**, 71 (2008). doi:10.1007/s11671-008-9119-3
20. T. Tsuru, Y. Shibutani, Atomistic simulation of elastic deformation and dislocation nucleation in Al under indentation-induced stress distribution. *Model Simul. Mater. Sci. Eng.* **14**, S55 (2006). doi:10.1088/0965-0393/14/5/S07
21. D. Saraev, R.E. Miller, Atomic-scale simulations of nanoindentation-induced plasticity in copper crystals with nanoscale-sized nickel coatings. *Acta Mater.* **54**, 33 (2006). doi:10.1016/j.actamat.2005.08.030